Demonstration of a saturated Ni-like Ag x-ray laser pumped by a single profiled laser pulse from a 10-Hz Ti:sapphire laser system

H. T. Kim,[1] I. W. Choi,[1] N. Hafz,[1] J. H. Sung,[1] T. J. Yu,[1] K.-H. Hong,[1] T. M. Jeong,[1] Y.-C. Noh,[1] D.-K. Ko,[1] K. A. Janulewicz,[2,*] J. Tümmler,[2] P. V. Nickles,[2] W. Sandner,[2] and J. Lee[1,†]

[1]*Advanced Photonics Research Institute, Gwangu Institute of Science and Technology, 1 Oryong-dong, Buk-gu, 500-712 Gwangju, Republic of Korea*

[2]*Max Born Institute, Max-Born-Strasse 2A, D-12489 Berlin, Germany*

(Received 4 May 2007; revised manuscript received 19 October 2007; published 6 February 2008)

A variant of a grazing-incidence pumping (GRIP) scheme for Ni-like x-ray lasers using a single shaped pulse from a 10-Hz Ti:sapphire laser system has been demonstrated. Experimental and numerical results show that efficient excitation leading to the lasing process can be achieved by controlled shaping of the pump laser pulse. Such a pulse has been defined for a silver slab target. A gain coefficient as high as 76 cm^{-1} was estimated. Results indicate that the nanosecond amplified spontaneous emission background of the leading edge of the driving pulse is decisive for an efficient pumping process in this version of GRIP.

DOI: 10.1103/PhysRevA.77.023807 PACS number(s): 42.55.Vc, 32.30.Rj, 42.60.By, 52.50.Jm

I. INTRODUCTION

A significant amount of effort during the last decade has been dedicated to the development of table top repetitive x-ray lasers. Specifically, significant progress has been reported in reducing the necessary pumping energy for soft x-ray lasers based on the Ni-like isoelectronic sequence. Starting from breakthrough experiments that used an energy of 5–7 J to pump a Ni-like medium [1,2], the amount of energy needed to saturate Ni-like x-ray lasers has been systematically reduced to 1 J [3]. The latest step in their development has been made possible by a pump geometry called grazing-incidence pumping (GRIP), proposed [4] and demonstrated by the Livermore group [5]. The efficiency of this arrangement has been confirmed by experiments reported in [3,6]. In spite of having a much lower pump energy, the recorded gain coefficient increased significantly in comparison with a traditional scheme using normal incidence and achieved values between 50 and 70 cm^{-1} [3,5]. Very recently, the physical basis of x-ray lasers pumped in the GRIP geometry has been comprehensively elucidated in [7,8], using quasianalytic methods and scaling rules supported by a series of numerical simulations.

In the transient inversion scheme, the pumping geometry usually uses two beamlines, one to deliver a preforming pulse in order to create plasma of the required ionization stage, with the second beamline transporting a main pulse to rapidly heat the preformed plasma and generate the required population inversion. Application of a single profiled pump laser pulse was one of the methods used to reduce the required pump energy and to simplify the pump geometry of the traditional double-pulse scheme of normal incidence [9]. The profiled pump pulse was formed in a Nd:glass laser system, and only the shape of the trailing edge was modified and analyzed in detail [13].

In this paper, we report on a variant of the GRIP geometry applied to a Ni-like Ag x-ray laser. The x-ray laser was pumped by a single profiled laser pulse from a 10-Hz Ti:sapphire laser system. Using the optimized pump laser pulse structure, we succeeded in saturating a Ni-like Ag x-ray laser with a very high gain. Estimated values of the output energy and beam divergence were 1.5 μJ and 4 mrad, respectively. The reduction from two pump laser pulses to only one, by means of controlled pulse shaping, brings noticeable benefits to the experimental arrangement. First of all, energy deposition is improved by perfect spatial overlapping of the precursor creating preplasma and the component responsible for heating of the plasma. In this way, inherent problems associated with the pointing of a pump laser beam can be eliminated. This is especially important for GRIP geometry because the usual widths of the focal line in this scheme do not exceed 30 μm.

II. EXPERIMENTAL SETUP

The experiment was performed by using a 100-TW laser facility at the Advanced Photonics Research Institute (APRI). The 100-TW Ti:sapphire laser system used in this experiment can deliver laser pulses of 30 fs pulse duration and 3 J laser energy, operating at a 10-Hz repetition rate. In the experiment on a Ni-like Ag x-ray laser, an 8-ps [full width at half maximum (FWHM)] laser pulse, stretched from the standard value, with 1.5 J of energy, irradiated the target at a grazing angle of 18°. Astigmatism of the focusing spherical mirror with a focal length of 75 cm was used to create a 7.2-mm-long focal line on the target. Here, the width of the focus was estimated to be about 30 μm (FWHM). A slab target with a width of 7 mm was used in the experiment, with the possibility to vary the length of the active medium irradiated by the pump pulse. The method for target length variation needs a brief comment. As a profiled target of variable length was not at our disposal, a rectangular target was moved parallel to its surface in the direction opposite to the spectrometer. This method might appear to be questionable. However, the length of the focus for each shot was determined by microscopic measurement of the crater length left on the target surface. It was found that the uncertainty of the

*kaj@mbi-berlin.de
†leejm@gist.ac.kr

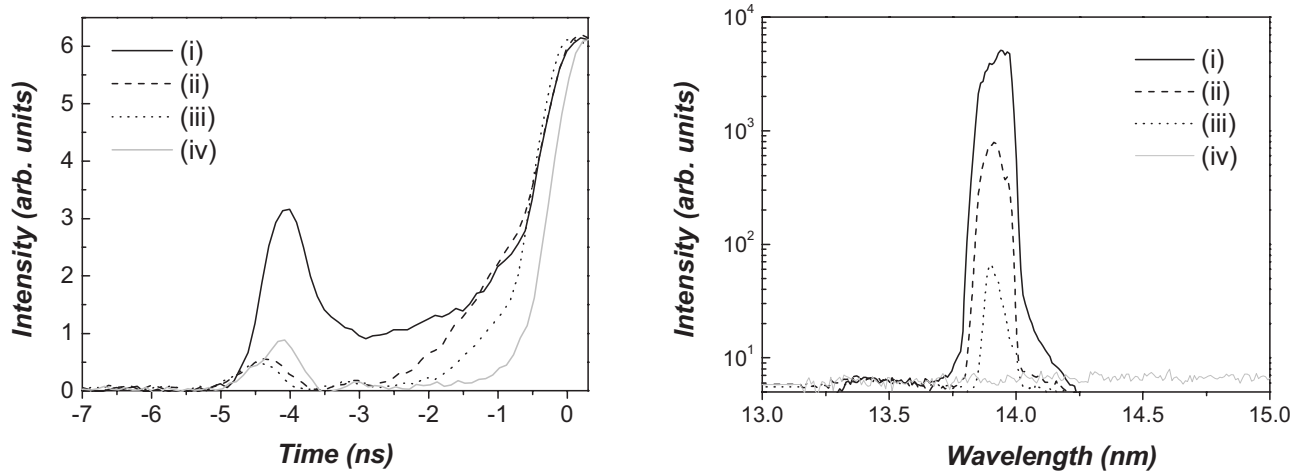

FIG. 1. (a) Changes of the temporal profile of the uncompressed laser pulses by manipulation of the Ti:sapphire laser system. (b) Changes in the spectrum of the x-ray laser output corresponding to the changes of the laser profile.

length was less than 0.2 mm. It should be noted that the line focus in the GRIP geometry is achieved by astigmatic focusing of the pump laser beam. The focal line does not have the spindle shape typical for lateral irradiation of the target. The irradiation is very sensitive to the angle of incidence and usually falls off very quickly outside the beam waist. This made possible the quoted reasonable accuracy in determination of the focus length. The reliability of the measurement method was also supported by the result of fitting of the experimental data. Assuming some uncontrolled additional length of the focus line contributing to the output signal in the case of the target shift, one should observe clear overestimation (increase) of the signal for short plasma columns. Then this uncontrolled contribution would be comparable to that resulting from the focus line of length assumed to be known. Itwould create difficulties (unpredictable inflection) in fitting the data and somewhat reduce the small-signal gain coefficient. However, none of this was observed in the data processing, and we assumed the measurement method to be reliable in this specific case. The average linear fluence was 215 mJ/mm. The deflected output of the soft x-ray radiation was aligned by deliberate tilting of the slab target (up to 5 mrad), to compensate refraction and properly enter a flat-field spectrometer (FFS) [10]. The FFS has a small acceptance angle of about 5 mrad. The FFS was equipped with a cylindrical collecting mirror, a 512×2048 pixel charge-coupled-device (CCD) camera, and a set of zirconium (Zr) filters. No fine slit was used in the spectrometer.

III. PULSE SHAPING

The pump arrangement takes advantage of a specific structure of the driving-pulse leading edge. This structure includes a low-level ($\sim10^{-3}I_{\max}$) precursor falling on the target at grazing incidence, to prepare the plasma for the subsequent heating process occurring after absorption of a strong ($I_{\max}$) picosecond main component of the pulse, incident at the same angle. The two components are separated by about 4 ns and overlap a low-level ($\sim10^{-5}I_{\max}$) pedestal (background) of a length comparable with the separation of the pulses, originating in amplified spontaneous emission (ASE).

The shaped pump laser pulse was formed by controlling the injection process at the regenerative amplifier positioned at the front end of the pump laser system and by controlling the delays between the amplifier stages. In a Ti:sapphire laser system using a regenerative amplifier at the front end of the system, the profile of the output laser pulse intrinsically contains a prepulse (precursor) and an ASE component at the leading edge. This prepulse has the same duration as the main component and precedes the latter by a constant time interval of a few nanoseconds. The ASE component of the leading edge, typically with a duration of a few nanoseconds, spans the gap between the precursor and the main component of the pump laser pulse. Figure 1(a) presents the temporal profiles of the driving laser pulse in front of the compressor. After the compressor, the temporal profile of the driving pulse [curve (i) in Fig. 1(a)] can be shaped to the form shown in Fig. 3. The latter was employed in the numerical simulations. Such a pulse includes a prepulse of controlled level and the ASE component of variable level and duration. The laser profiles presented in Fig. 1 were measured using a fast photodiode with a 350-ps response time. The signal of the

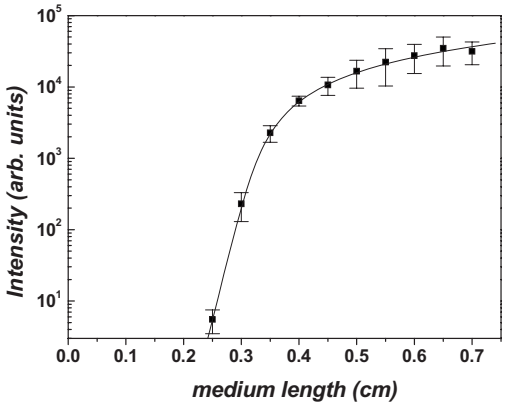

FIG. 2. X-ray laser output signal vs medium length.

main component from the photodiode was saturated to observe the low-intensity part of the leading edge of the laser pulse. The duration of the main pulse and prepulse was reduced to ~8 ps after the compression process. The ASE level of the pulse after compression was confirmed through measurements with a third-order correlator (SEQUOIA, Amplitude Technology). It was found that the ASE level from the third-order correlator was about 10^{-5} times the magnitude of the intensity of the main component as the latter increased about 40 times due to compression. However, the prepulse was also compressed, and its overall intensity was actually about 10^3 times lower than that of the main component. The peak intensity of the main part of the pulse was estimated to be about 9×10^{13} W/cm^2.

IV. MEDIUM KINETICS

A drastic increase in the output signal of the x-ray laser was observed with corresponding increases in both the prepulse level and the length and level of the spontaneous emission component of the leading edge [compare Figs. 1(a) and 1(b)]. This result is not surprising, as an increase of the prepulse level enlarges the volume of the active medium (plasma plume) while ASE is responsible for further energy delivery to the plasma and keeping it close to optimum conditions for the forthcoming heating by the intense, main pulse component. This scenario reflects well the general requirements for the pump process formulated in [7]. However, there is an optimum energy that needs to be delivered in the prepulse and the ASE pedestal. As the prepulse creates a low-volume plasma column, an overly strong ASE can bring it closer to the optimum ionization level, and then the main intense pulse component has the potential to significantly overionize the medium; as a consequence, gain would be reduced. It was observed during the experiment that an increase in energy of the ASE pedestal by one order of magnitude reduced the output signal by nearly two orders of magnitude, precluding any strong saturated lasing.

This trend was qualitatively confirmed by the computations, where an increase of the flat-top pedestal level by one order of magnitude changed the average ionization stage of the preionized plasma in the subsequent high-gain zone from 1.85 to 9.4 and moved the high-gain area about 6 μm towards the target—that is, in the region of steeper density gradients. Moreover, even if the maximum local gain coefficient was comparable in both cases, the stronger ASE pedestal caused the diameter of the high-gain area to be reduced by a factor of 2.5, and thus any strong lasing was hindered. In contrast, a very weak ASE will leave the preplasma too far from the optimum state and without a well-developed plasma column. As a result, the ionization stage cannot be optimized during the heating component of the pulse and the propagation conditions in the underdeveloped plasma column preclude any lasing. The preplasma parameters calculated at the future positions of the maximum gain confirm this scenario. It was found that absence of the ASE pedestal causes the preplasma at the onset of the main part of the pump pulse to have a density well below 10^{19} cm^{-3}, an ionization stage equal to 0.11, and an electron temperature below 0.1 eV. The preplasmas produced by a pump laser pulse without the prepulse, but with ASE, and by the pump laser pulse including both prepulse and ASE are quite similar. The plasma densities are 7.5×10^{19} cm^{-3} and 5.5×10^{19} cm^{-3}, the ionization stages are 1.81 and 1.85, and the temperatures are 4.05 eV and 3.97 eV for each variant, respectively. However, in the pump version including all components, the maximum gain has been achieved at a distance from the target that is longer by a factor of 2 in comparison to that when only the ASE preforms the medium.

The output x-ray laser signal in the experiment was maximized by the previously mentioned driving laser profile control procedure. When the leading edge of the laser pulse changed, a significant increase of the x-ray laser signal was observed. The signal strengthening was correlated with the increase in the ASE duration, up to the full span of the prepulse and the main heating component of the laser pulse. This is clearly seen from Fig. 1; pulses (ii) and (iii) in Fig. 1(a) have similar prepulse intensities, whereas the ASE starts to grow at different moments. The x-ray laser signal increased more than 10 times as a result of elongation of the ASE pedestal, as seen in Fig. 1(b). Consequently, saturation of the x-ray lasing signal was achieved when the controlled laser pulse had the profile denoted as line (i) in Fig. 1(a). For the optimum laser profile, the prepulse and main heating pulses were connected by the ASE background. The x-ray laser spectrum shown in Fig. 1(b) was broader than the real linewidth of the emitted radiation due to the lack of a fine entrance slit in front of the FFS.

A. Gain measurement

A careful characterization of the x-ray laser output signal with variation of the medium length was performed to quantify the gain behavior of the system pumped in this unconventional way. Figure 2 shows the x-ray laser output signal with respect to the target length. Each point of the scatter represents an average value of a few shots, and the error bars show the range between the maximum and minimum values used in the averaging process. To avoid controversy connected with the choice of the interpolation range, we determined the gain coefficient using the modified Linford formula proposed in [11]. For the Gaussian gain profile, the output of the x-ray laser with respect to the target length can be determined by two equations as follows [11]:

$$I_L = I_0\alpha(GL) = I_0\frac{(e^{GL}-1)^{3/2}}{(GLe^{GL})^{1/2}}, \tag{1}$$

$$G_0L = \left(1-\frac{I_0}{I_s}\right)GL + \frac{I_0}{I_s}\alpha(GL), \tag{2}$$

where I_L is the output x-ray laser intensity, L is the length of the medium, G is the saturated gain, and G_0 is the small-signal gain coefficient. I_0 is the total spontaneous emission, and I_S is the saturation irradiance. I_0,I_S, and G_0 are assumed to be constant along the plasma and during the x-ray laser transit time. An approximate value of G_0 was obtained by nonlinear fitting of the Linford formula to the first two data

points, where the x-ray intensity increases exponentially with target length. Then, using Eqs. (1) and (2), we made a complete fit of the x-ray output with respect to the target length. The fitting by using these equations matches very well the x-ray laser output measured in the experiment, as shown in Fig. 2. The values estimated by fitting the average data points gave 76 cm^{-1} for the small-signal gain coefficient and 28.2 for the effective gain-length product. However, it has to be stressed that the gain values calculated by ray tracing were significantly higher and exceeded 100 cm^{-1}. This measured value is a little bit higher than that reported in [14] for a slightly weaker pumped Ni-like silver laser. Note that though the increase in the signal intensity observed for the first two or three points is of one order of magnitude, intensity strengthening for the whole medium length amounts to five orders of magnitude. Thus, it can be confirmed that the small-signal gain coefficient measured in the experiment is very high. Clear saturation-caused roll-off of the curve begins at a target length of 3 mm. Consequently, the saturated operation of a Ni-like Ag x-ray laser pumped by a single shaped pulse from a Ti:sapphire laser system is irrefutable.

B. Numerical modeling

The EHYBRID code developed at York University [8,12] was used in the simulations conducted to give a theoretical basis for the experiment on this pump method. This code describes plasma development in one direction through a self-similarity solution, and for this reason it is denoted as a 1.5D code. It is possible that the very narrow focal lines used in these GRIP experiments need a full two-dimensional description to provide more reliable values for the plasma dynamics and resulting plume dimensions. Nevertheless, this code proved to be very reliable as far as the description of the kinetics in an x-ray laser medium is concerned [7,13].

Figure 3 shows the modeled pulse shape used in the simulations and reflects the profile deduced from the measurements with the fast photodiode and the third-order correlator. Gaussian shapes with widths of 8 ps (FWHM) were used for both the prepulse and the main heating pulse. The nanosecond spontaneous emission component was partly modeled with a flat-top shape. Some part of the ASE component was, for technical reasons, included in the lengthened wing of the main-pulse leading edge. The peak of the heating pulse was fixed at a position of 4 ns after the irradiation onset. The total energy on the 7-mm-long target was 1.5 J. The energies contained in the ASE component and prepulse were 6.1 mJ and 2.7 mJ, respectively; hence, the total energy delivered before the main pulse arrival was about 9 mJ. These values were estimated from the geometrical relations of the shape modeled for the simulations. Real values are most likely slightly higher as the amount of energy contained under the long wing of the leading edge is unknown. We assumed that it could double the amount of energy calculated from the geometrical shape. If the pulse shape was optimized for maximum lasing, the shot-to-shot fluctuation of the energy in the leading edge of the pump-laser pulse observed in the experiment was between 20% and 50%. Note that even the maximum possible signal gives an extremely small amount of energy, and some uncertainties due to the paucity of data for equations of state at such low energies could quantitatively influence the calculated values of the plasma dimensions.

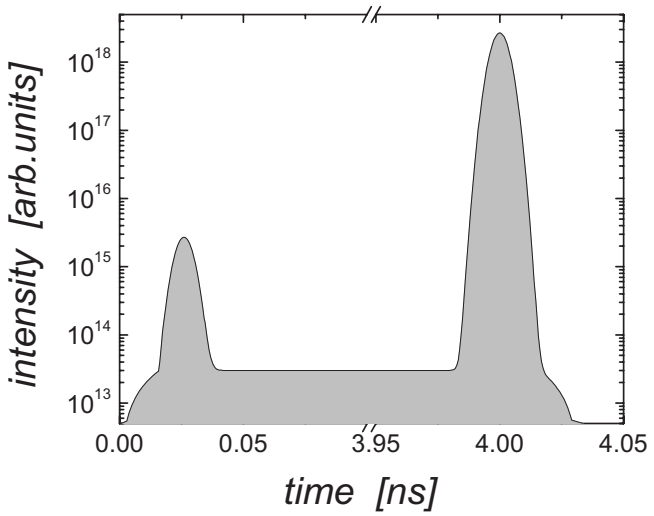

FIG. 3. Temporal profile of the pump pulse used in the simulations described in the text. Note the logarithmic scale used to provide detailed information about the pulse shape at low levels of intensity. The time scale is divided into two separated parts, omitting an extended featureless section. Both spikes have a width (FWHM) of 8 ps.

The results of the experiment presented a clear correlation between the different shapes of the pump laser pulse and the output of the Ni-like silver x-ray laser, as shown in Fig. 1. It was found that the ASE pedestal and the leading edge shape are more influential than the prepulse level for the lasing process. It was important to confirm if these correlations were also present in the modeled experiment. Therefore, three cases were used: the optimum laser profile with the prepulse and the ASE pedestal, the pulse profile without prepulse, and the pump pulse without the ASE background. Figure 4 shows the spatiotemporal development of the local gain coefficient calculated for the described pulses. Figures 4(a) and 4(b) show the local gain in the case without the ASE component and without the prepulse, respectively. Without the nanosecond-long background originated in the ASE [Fig. 4(a)], the gain is almost not visible in the required area and it is short-lived. This situation corresponds to some extent to the curve (iv) in Fig. 1(a) recorded in the experiment. It is clear that this precludes any noticeable lasing, as the x-ray laser beam sampling the medium will be very quickly deflected from the tiny active volume. As the prepulse is of picosecond duration, both the material ablation and the active volume are very limited. The absence of the ASE component leaves a small amount of relatively cold plasma without the additional source of energy present in the optimum case. The plasma plume expands, but it will be cooled rather than heated before the onset of the main component. This explains the crucial role of the ASE pedestal in the pump process.

Reasonable lasing is not hindered by the removal of the prepulse [Fig. 4(b)], as it exists in a distinctive high-gain area that changes its position with time. This in turn causes

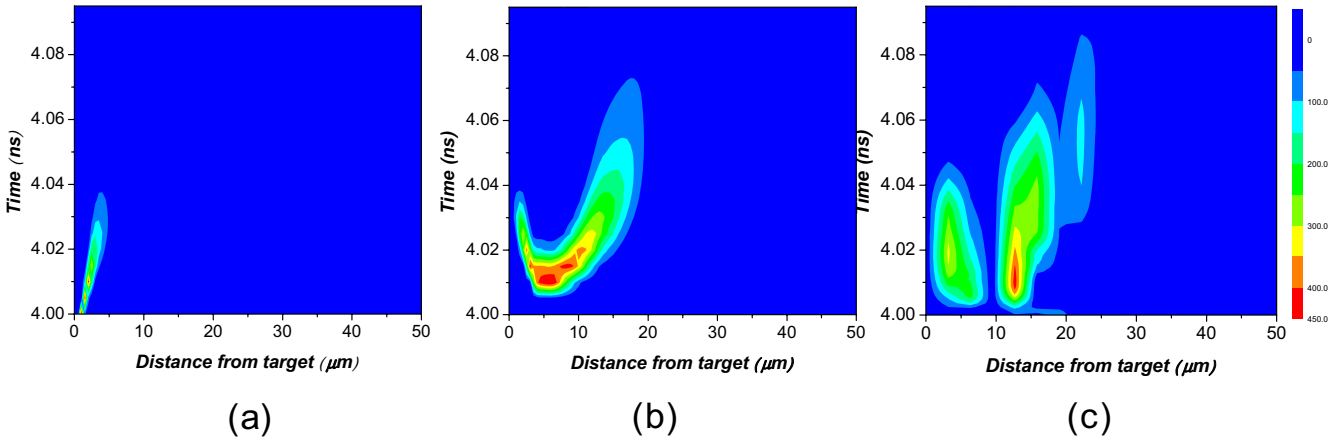

FIG. 4. (Color online) Spatiotemporal profiles of local gain coefficients from simulations with the EHYBRID code in the case of (a) without the ASE, (b) without the prepulse, and (c) with all components (prepulse, ASE, and main pulse). The gain scale given by the vertical bar is labeled in cm^{-1}.

propagation effects to be important in limiting the amplification process. In the case of the shaped pulse including all three components, Fig. 4(c) presents the broadest area of high gain, split in space, but at a position unchanged with time. The spatial stability and volume of the high-gain area provide an important advantage for energy extraction as it reduces the refraction-induced losses. The split of the gain area is caused by overionization of the active medium near the target surface. Figure 4(c) also shows that the strong prepulse enlarges the high-gain area and produces a stronger x-ray laser output of better quality, provided that the main component is sufficiently strong. Consequently, a profiled pulse containing a prepulse and a nanosecond spontaneous emission pedestal in the leading edge can effectively create x-ray lasing, as shown in the experimental results and accompanying theoretical simulations.

V. SUMMARY

In conclusion, we have shown by experiments and by simulations that pumping of an x-ray laser medium with a single profiled laser pulse is possible in GRIP geometry. A very high gain coefficient has been recorded in our experiments. In addition, the simulations clearly show that the most critical parameter in the single profiled pumping scheme is the nanosecond background of the spontaneous emission. This simple pump method with a single profiled pulse can be especially important in abbreviating the injector-amplifier scheme, where the number of overlapped pump pulses can be reduced by pump pulse shaping, with a stabilizing effect for the position and volume of the amplifying medium. An output beam of good quality demonstrated in the experiment suggests reduced density gradients in the plasma column, and this suggests favorable prospects for the generation of a high-quality and strongly coherent output beam in the injector-amplifier system. Further work on this scheme is in progress.

ACKNOWLEDGMENTS

It is a pleasure to acknowledge helpful discussions with Professor G. J. Pert from the University of York and continuous support from Professor Chang Hee Nam (KAIST) for the cooperation between MBI and APRI. This work is supported by the Ministry of Commerce, Industry, and Energy of the Republic of Korea through the "Core Technology Development Program." The members of the MBI group gratefully acknowledge support during this work by the International Office of BMBF (Grants Nos. KOR 06/014 and KAP 05/003) within the German-Korean Collaboration Program.

[1] J. Dunn, A. L. Osterheld, R. Shepherd, W. E. White, V. N. Shlyaptsev, and R. E. Stewart, Phys. Rev. Lett. **80**, 2825 (1998).
[2] J. Dunn, Y. Li, A. L. Osterheld, J. Nilsen, J. R. Hunter, and V. N. Shlyaptsev, Phys. Rev. Lett. **84**, 4834 (2000).
[3] B. M. Luther, Y. Wang, M. A. Larotonda, D. Alessi, M. Berrill, M. C. Marconi, J. J. Rocca, and V. N. Shlyaptsev, Opt. Lett. **30**, 165 (2005).
[4] R. Keenan, J. Dunn, V. N. Shlyaptsev, R. F. Smith, P. K. Patel, and D. F. Price, Proc. SPIE **5197**, 213 (2003).
[5] R. Keenan, J. Dunn, P. K. Patel, D. F. Price, R. F. Smith, and V. N. Shlyaptsev, Phys. Rev. Lett. **94**, 103901 (2005).
[6] J. Tümmler, K. A. Janulewicz, G. Priebe, and P. V. Nickles, Phys. Rev. E **72**, 037401 (2005).
[7] G. J. Pert, Phys. Rev. A **73**, 033809 (2006).
[8] G. J. Pert, Phys. Rev. A **75**, 023808 (2007).
[9] K. A. Janulewicz, A. Lucianetti, G. Priebe, W. Sandner, and P. V. Nickles, Phys. Rev. A **68**, 051802(R) (2003).
[10] I. W. Choi, J. U. Lee, and C. H. Nam, Appl. Opt. **36**, 1457 (1997).
[11] J. Y. Lin *et al.*, Opt. Commun. **158**, 55 (1998).

[12] P. B. Holden, S. B. Healy, M. T. M. Lightbody, G. J. Pert, J. A. Plowes, A. E. Kingston, E. Robertson, C. L. S. Lewis, and D. Neely, J. Phys. B **27**, 341 (1994).
[13] K. A. Janulewicz, J. Tümmler, G. Priebe, and P. V. Nickles, Phys. Rev. A **72**, 043825 (2005).
[14] Y. Wang, M. A. Larotonda, B. M. Luther, D. Alessi, M. Berrill, V. N. Shlyaptsev, and J. J. Rocca, Phys. Rev. A **72**, 053807 (2005).